

LINEAR AND NONLINEAR COUPLINGS BETWEEN
ORBITAL FORCING AND THE MARINE $\delta^{18}\text{O}$ RECORD
DURING THE LATE NEOGENE

Teresa Hagelberg and Nick Piasis

College of Oceanography, Oregon State University, Corvallis

Steve Elgar

Department of Electrical Engineering and Computer Science,
Washington State University, Pullman

Abstract. Previous investigations of the response of Plio-Pleistocene climatic records to long-term, orbitally induced changes in radiation have considered a linear response of climate. While the second-order statistics of power spectra and cross spectra provide necessary information on linear processes, insight into the nonlinear characteristics of Pliocene and Pleistocene climate is not provided by these statistical quantities. Second-order statistics do not contain the phase information necessary to investigate nonlinear, phase-coupled processes. Such information is provided by higher-order statistical quantities. In particular, bispectral analysis indicates that nonlinear couplings are present in the climatic (radiative) forcing at the Milankovitch frequencies. Through a linear transfer, this forcing produces similar nonlinear couplings in deep-sea sedimentary oxygen isotope records (ODP site 677 and DSDP site 607) from 1.0 to 0 Ma during the late Neogene. This analysis suggests that during the late Pleistocene, the dominance of the 100,000 year cycle in the climate record is consistent with a linear, resonant response to eccentricity forcing. In the period from 2.6 to 1.0 Ma, a change in the nature of the climatic response to orbital forcing is indicated, as phase couplings present in the isotopic time series are not similar to the phase couplings present in the insolation forcing. Third-order moments (skewness and asymmetry) are used to quantify the shape of the climatic response. From 2.6 Ma to present, an increase in the asymmetry (sawtoothness) of the oxygen isotopic records is accompanied by a corresponding decrease in the skewness (peakedness) of the records. This indicates an evolution in the nature of the phase coupling within the climate system. These results may provide important constraints useful in development of models of paleoclimate.

Copyright 1991
by the American Geophysical Union.

Paper number 91PA02281.
0883-8305/91/91PA-02281\$10.00

INTRODUCTION

Since the pioneering work of Hays et al. [1976], researchers have successfully identified a linear response of Plio-Pleistocene climate to orbital forcing [e.g., Piasis and Moore, 1981; Imbrie et al., 1984, 1989; Raymo et al., 1989; Ruddiman et al., 1989], supporting the Milankovitch hypothesis of climate change. Empirical evidence in support of this hypothesis is strengthened by observations of high coherence and relatively constant phase between the climatic forcing (orbital tilt and precession) and the response (global ice volume) at periods of 41, 23 and 19 kyr. These results suggest a linear relationship between ice sheet growth and decay and orbitally induced changes in the distribution of solar radiation.

A linear response of the climate system to solar insolation changes can account for much of the variance in the obliquity (41 kyr) and precession (23-19 kyr) bands of the paleoclimate spectrum, but it is generally thought to be insufficient to explain the dominance of the 100 kyr cycle during the Pleistocene [Imbrie et al., 1989 and references therein]. Efforts to explain the dominance of 100 kyr power in the paleoclimate record have produced a range of results, as discussed below.

Studies which contend that a linear response cannot explain the 100 kyr cycle in the paleoclimatic record often argue that insolation forcing in the 100 kyr eccentricity band is too small to produce the observed response or that it is altogether nonexistent [e.g., Imbrie et al., 1989; Birchfield and Weertman, 1978]. Although the direct influence of eccentricity on insolation is small (of the order of 0.1% [Berger, 1977]), eccentricity is the only orbital parameter that influences the total amount of radiation the Earth receives annually [Berger, 1989]. In addition, eccentricity variations are observed to correlate positively with changes in estimated summer temperature [Berger, 1978a, Hays et al., 1976]. It is still unknown whether the paleoclimatic spectral peak at 100

kyr is produced from (1) a linear response to eccentricity or (2) a nonlinear interaction between two precession band oscillations which transfers energy to the 100 kyr band. To investigate this problem, the relative proportions of variance in the paleoclimatic record that are related to a linear response to eccentricity and to a nonlinear response to precessional forcing must be determined.

Paleoclimate research in this area has proceeded along two similar avenues. On one hand, analyses of geologic data provide fundamental observations of how climate has varied over the past several million years. Successful, extensive strategies have been developed to examine records within a consistent chronologic framework and in a systematic manner [e.g., Imbrie et al., 1989]. On the other hand, models have been developed which seek to describe the physics governing these changes with varying degrees of complexity (see the summary by Saltzman [1985, and references therein]). Deterministic models describing dynamics of the "slow response" of climate system evolution are divided into two groups by Saltzman [1985]: (1) quasi-deductive models, based on prognostic equations for specific processes [e.g., Birchfield and Weertman, 1978; Birchfield and Grumbine, 1985; Le Treut and Ghil, 1983; Oerlemans, 1982; Pollard, 1983; Peltier, 1982] and (2) inductive models, which attempt to construct a dynamical system of equations, based on known physical feedbacks, from which reasonable paleoclimatic output can be produced [e.g., Imbrie and Imbrie, 1980; Saltzman and Sutera, 1984; Saltzman et al., 1984; Maasch and Saltzman, 1990]. Several models (of both types) invoke a nonlinear response of the climate system to ice sheet formation to explain the 100 kyr cycle [Le Treut and Ghil, 1983; Imbrie and Imbrie, 1980; Wigley, 1976; Birchfield and Weertman, 1978; Sneider, 1985]. Other models explain this cycle as a free oscillation of the climate system, whose phase is set by weak eccentricity forcing [Saltzman and Sutera, 1984; Saltzman et al., 1984]. Finally, a few models incorporate stochastic effects [Hasselmann, 1976; Matteucci, 1989].

Thus a wide range of classes of models exist, all of which seek to explain the same phenomenon (Pleistocene climate). A general test of each model is its ability to reproduce characteristics that are present within the data, as well as its ability to predict characteristics which have not yet been (or cannot be) determined from data. To first order, every model reproduces some feature or features of the paleoclimatic record, most commonly its power spectrum (a second-order statistic). Insights into the higher-order statistics of the data can provide additional constraints or tests for evaluating the models.

Although some observations suggest a nonlinear response of the paleoclimate system to orbital forcing, this response has not been quantified, in part because the power spectrum does not contain phase information. Power spectral analyses are incapable of detecting the phase coupling which characterizes a nonlinear interaction. Similarly, the cross spectrum contains phase information between only two records at a given frequency and is therefore capable of resolving only a linear relationship. Both the power spectrum and cross spectrum are derived from covariance, a second-order statistical quantity. The presence of quadratic nonlinear interactions between oscillations of different frequencies can be addressed most effectively through the use of the bispectrum, a third-order statistical quantity.

In this study, bispectra of the time series of orbitally induced insolation changes and time series of the oxygen isotopic proxy of global ice volume (from ODP site 677 and DSDP site 607) are presented. Cross spectra and bispectra are used to show that both the radiative forcing and the climatic response contain nonlinearly coupled components, but the interaction between the insolation forcing and response is primarily linear. The analysis suggests that the 100 kyr power observed in the paleoclimatic record is consistent with a linear, resonant response to insolation forcing.

First, a brief introduction to bispectral analysis, including a simple example, is presented. Next, the bispectra of the calculated record of radiative forcing as well as three Plio-Pleistocene records of global ice volume ($\delta^{18}\text{O}$) are presented. The time period from 1.0 to 0 Ma, where 100 kyr power is very high, is compared to the period from 2.6 to 1.0 Ma, where 100 kyr power is lower. Higher-order moments (skewness and asymmetry) are shown to provide quantitative insights into features of these records. Finally, the implications of these results for paleoclimate model development is examined.

BACKGROUND

Bispectral techniques have been in use for over 25 years [Hasselmann et al., 1963] (see also the review by Nikias and Raghuveer [1987]). Because this is the first application of these techniques to paleoclimatic time series, a brief summary and an example of its application are presented.

The bispectrum is formally defined as the double Fourier transform of the third-order autocorrelation of a time series [Hasselmann et al., 1963]. While the power spectrum describes the distribution of variance (the second central moment) as a function of frequency, the bispectrum describes the distribution of the third moment as a function of bi-frequency. For a discretely sampled time series $x(t)$ with complex Fourier coefficients at frequency f_j given by $X(f_j)$, the power spectrum is

$$P(f_j) = \langle X(f_j) X^*(f_j) \rangle \quad (1)$$

where the angled brackets indicate expected value (mean) and the asterisk indicates complex conjugate. Similarly, the bispectrum is given by [Haubruch, 1965; Kim and Powers, 1979]:

$$B(f_j, f_k) = \langle X(f_j) X(f_k) X^*(f_j+f_k) \rangle \quad (2)$$

If there is energy (variance) at frequency f_j , then $P(f_j)$ is nonzero. The bispectrum, however, is zero at the bi-frequency f_j, f_k , when the modes f_j, f_k , and f_j+f_k are independent of one another, even if energy is present at these frequencies. For independent oscillations, the phases are random relative to each other, yielding a zero bispectrum upon averaging over many realizations. In theory, the bispectrum is nonzero only if these three modes are quadratically coupled, meaning that their phases are nonlinearly coupled to one another.

Like the cross spectrum, which provides coherence and phase information, the complex-valued bispectrum is often cast in terms of its normalized magnitude, the bicoherence, and its phase, the biphas (denoted $b(f_j, f_k)$ and $B(f_j, f_k)$, respectively). The squared value of bicoherence, $b^2(f_j, f_k)$, represents the

fraction of power at frequency $f_j + f_k = f_{j+k}$ owing to quadratic (nonlinear) interactions of the three modes [Kim and Powers, 1979]. Analogous to the linear coherence spectrum, the bicoherence spectrum is normalized such that $0 \leq b \leq 1$ [Kim and Powers, 1979]. The biphase is analogous to the phase of the cross spectrum, and ranges between $-\pi$ and π .

A simple example demonstrates the effect of nonlinear phase coupling on both the shape of a time series and the detection of phase coupling by the bispectrum. Let the time series $x(t)$ be composed of three cosines and a low-amplitude Gaussian noise component:

$$x(t) = \cos(2\pi f_1 t + \phi_1) + \cos(2\pi f_2 t + \phi_2) + \cos(2\pi f_3 t + \phi_3) + \text{noise} \quad (3)$$

where f_i is the frequency and ϕ_i is the phase of each cosine.

The frequencies of these cosines are chosen to be $f_1 = 0.010$, $f_2 = 0.043$, and $f_3 = f_1 + f_2 = 0.053$ for ease in comparison of this simulated record with late Pleistocene $\delta^{18}\text{O}$ time series, which show power spectral peaks at these frequencies in cycles/thousand years. Three different cases are examined. In the first case (case 1), ϕ_1 , ϕ_2 , and ϕ_3 are all random variables uniformly distributed over $(0, 2\pi)$. This case represents a linear (Gaussian) system where there is no nonlinear phase coupling. The phases of each oscillation are random relative to one another when averaged over many realizations. In the second case (case 2), ϕ_1 and ϕ_2 are uniform random variables, but $\phi_3 = \phi_1 + \phi_2$, and thus f_1, f_2 , and f_3 are now phase coupled. The relationship between the three modes is no longer random. Similarly, in the last case (case 3), ϕ_1 and ϕ_2 are uniform random variables, but $\phi_3 = \phi_1 + \phi_2 + \pi/2$ (the choice of ϕ_3 in cases 2 and 3 results in biphases of 0° and 90° , and waveforms with maximum skewness and asymmetry, respectively, as discussed below). For each case examined, 16 256-point realizations were made, resulting in a 4096-point record.

Portions of each time series and the corresponding power spectrum for each case are shown in Figures 1 and 2, respectively. In each case, the power spectra show concentrations of variance at frequencies f_1, f_2 , and f_3 with random fluctuations at other frequencies resulting from the noise. Even though the time series for each case look different, the power spectra are identical. This is because the power spectrum is phase independent and the three cases differ only in their phase relationships.

Figure 3 shows the bicoherence spectra for cases 1, 2, and 3. Smoothed power spectral and bispectral estimates were made by windowing (using a Hanning window) and averaging the 16 256-point ensembles for each record. Resulting estimates have 30 degrees of freedom (dof). The values contoured in Figure 3 are the observed bicoherences at the triad of frequencies $(f_1, f_2, f_1 + f_2)$ (denoted $b(f_1, f_2)$) which are significant at a $(1-\alpha) = 0.90$ level ($b_{90\%} = (4.6/\text{dof})^{1/2}$ [Elgar and Guza, 1988]). Owing to the symmetry properties of the bispectrum, it is necessary only to calculate the bispectrum within a triangular region defined by $0 \leq f_1 \leq f_N, f_2 \leq f_1$, and $f_1 + f_2 \leq f_N$, where f_N is the Nyquist frequency [Kim and Powers, 1979]. It is important to note that the direction of the nonlinear interaction is not given by the bispectrum, that is, sum interactions (interactions at f_1 and f_2 that produce $f_3 = f_1 + f_2$) are not distinguished from difference interactions (interactions at f_3 and f_2 that produce $f_1 = f_3 - f_2$, for example). This information

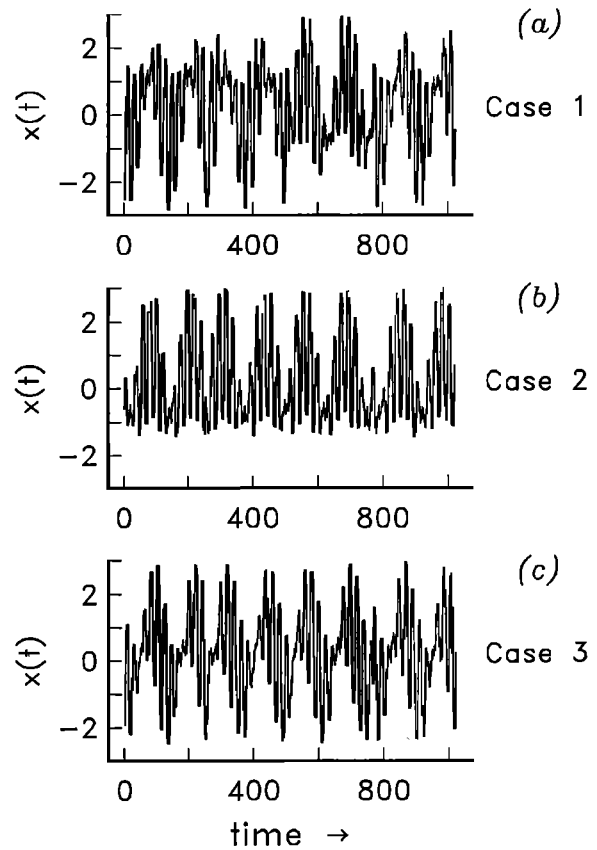


Fig. 1. Portions of each time series for cases 1-3 (see text): (a) case 1 ($f_1 + f_2 = f_3$; ϕ_1, ϕ_2, ϕ_3 are random), (b) case 2 ($f_1 + f_2 = f_3$; $\phi_1 + \phi_2 = \phi_3$), and (c) case 3 ($f_1 + f_2 = f_3$; $\phi_1 + \phi_2 = \phi_3 - \pi/2$). The units are arbitrary.

comes instead from other aspects of the physical system under examination, including the biphase [Kim et al., 1980; Elgar and Guza, 1985].

In case 1, the linear case in which no phase coupling is present, bicoherences near the triad $(0.059, 0.051, 0.110) = 0.370$ are significant at a 90% level (Figure 3a). Although all bicoherences in this case should be zero, any finite length time series will yield some nonzero values of bicoherence. This value of bicoherence represents the high values that can be expected to occur by random chance for a linear process with 30 dof. On the other hand, bicoherence at $(0.01, 0.043, 0.053)$ (the (f_1, f_2, f_3) triad) is 0.167, which is below the 90% significance level.

In cases 2 and 3, where phases are coupled, $b(0.01, 0.043) = 0.917$ and $b(0.01, 0.043) = 0.912$, respectively, indicating high bicoherence at the $(0.01, 0.043, 0.053)$ triad (Figures 3b and 3c). In case 2, the value of bicoherence indicates that at frequency 0.053, approximately 84% of the variance is quadratically coupled to the other two components of the triad. The value is less than 1.0 owing to the addition of noise.

Biphase estimates are related to the shape of the waveform (time series) [Masuda and Kuo, 1981; Elgar, 1987]. The waveform shape is often described by two normalized third

moments, skewness and asymmetry. Skewness is the normalized third moment of the time series and indicates asymmetry with respect to a horizontal axis, or top-bottom asymmetry. Asymmetry is the normalized third moment of the Hilbert transform of the time series [Elgar, 1987] and indicates asymmetry with respect to a vertical axis, or for-aft asymmetry. For a time series which is purely Gaussian, having only random phase relationships, the biphase is also random for every triad of frequencies.

In case 1 of the above example, the shape of the waveform is symmetrical, and skewness and asymmetry are zero. In Figure 1a, skewness = -0.12 and asymmetry = -0.16. The small nonzero third-moment estimates are caused by statistical fluctuations. In case 2, the biphase for the (0.01, 0.043, 0.053) interaction is zero, and the waveform is positively skewed (in Figure 1b, skewness = 0.80, asymmetry = 0). In case 3, the same triad has biphase of $\pi/2$, and the waveform is asymmetric or "sawtooth" shaped (in Figure 1c, skewness = 0, asymmetry = -0.79).

The asymmetric record of case 3 is qualitatively similar in shape to the SPECMAP stack (Figure 4), a smoothed

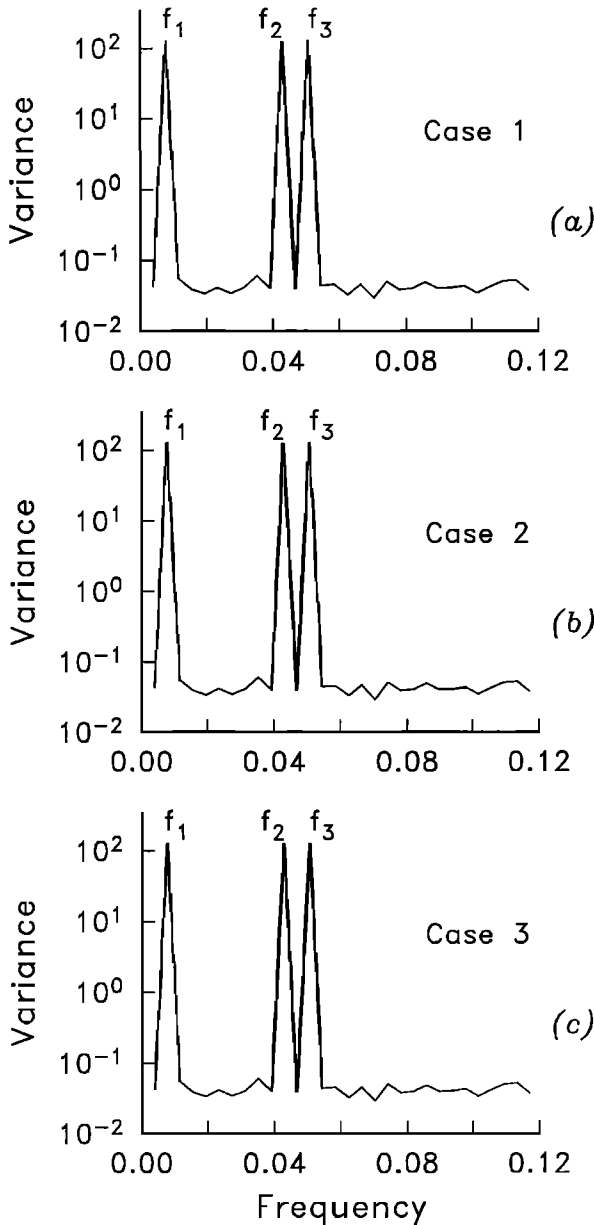


Fig. 2. Power spectra for cases 1-3. Smoothed power spectral estimates having 30 degrees of freedom were obtained using a Hanning window and by averaging 16 256-point ensembles for each record: (a) case 1, (b) case 2, and (c) case 3. The units are arbitrary.

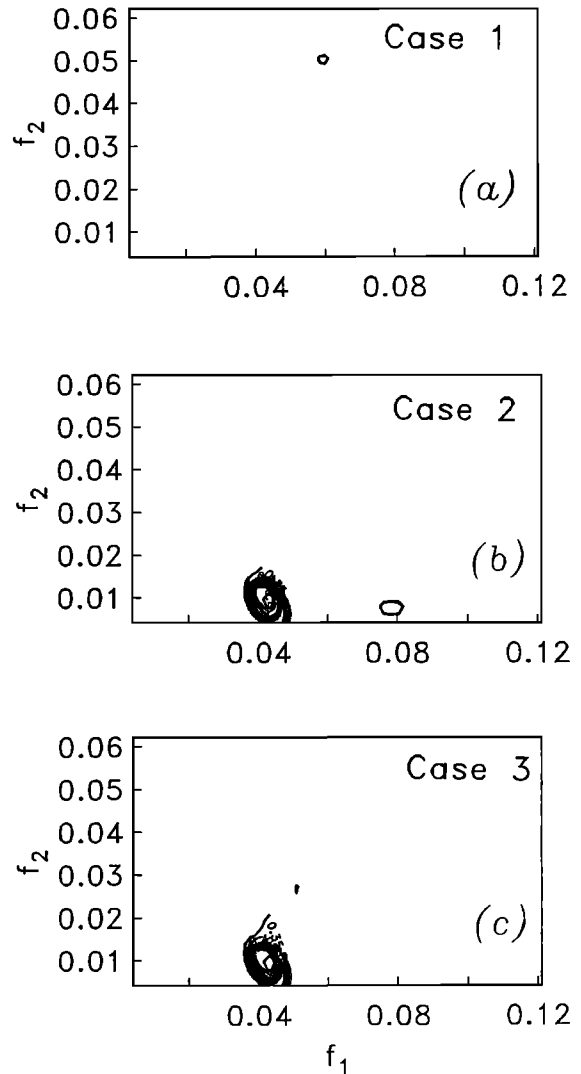


Fig. 3. Contours of bicoherence for cases 1-3. Smoothed bispectral estimates were obtained in the same manner as power spectral estimates and have 30 degrees of freedom. The minimum bicoherence value contoured (significant at a 0.90 level) is $b=0.39$ with additional contours every 0.05: (a) case 1, (b) case 2, and (c) case 3. The units of frequency are arbitrary.

composite record of five late Pleistocene ice volume ($\delta^{18}\text{O}$) records [Imbrie et al., 1984]. The SPECMAP record displays steep terminations representing the end of glacial stages, followed by a slow, gradual ice buildup. With minor adjustments to the record of case 3 (reduction of the amplitudes of f_2 and f_3) the resemblance to the SPECMAP stack is striking (Figure 4). The implications of this similarity are that quadratic phase couplings are of importance in the paleoclimatic record and that through the use of higher order statistics, these couplings can be quantified.

NONLINEAR COUPLINGS AMONG ORBITAL PARAMETERS

The bispectrum of the normalized time series of radiative (insolation) forcing (as calculated by Berger [1978b] is now examined. (Note that in this paper the 1978 solution of Berger is used. A more recent solution [Berger and Loutre, 1988] has been found to yield essentially the same results in the bispectrum as the older [Berger, 1978b] solution, although the orbital values in the new solution differ from the older solution in the time domain prior to 1 Ma. Because the values of the newer solution from 1.0 to 0 Ma are less well reproduced at present than those of the older solution, the 1978 values are used here.) Long-term (of the order of 100 kyr) variations in the Earth's insolation are produced through interacting motions of the Sun and planets relative to the Earth. At a given latitude on the Earth in a given season, the solar energy available is a function of the solar constant, the eccentricity of the Earth's orbit, the obliquity of the Earth's axis, and the longitude of perihelion as measured from the vernal equinox [Berger, 1978c].

Many studies have examined the paleoceanographic response to changes in these orbital parameters. Studying each orbital parameter separately has been considered reasonable as obliquity variations affect the latitudinal distribution of insolation, precessional changes affect the seasonal

distribution, and eccentricity variations affect the total insolation received over time. Examination of the terms that are used to derive long-term Earth orbital variations [e.g., Berger, 1978c] indicates that eccentricity, tilt, and precession [e , ϵ , and $e\sin\omega$] are indeed coupled to one another. However, no quantitative estimates of the strength of these couplings has been made. Bispectral analysis of the insolation record allows phase-coupled oscillations to be isolated.

A 4.096 m.y. record of July 65°N radiation sampled at 2000 year intervals is shown in Figure 5a. The power spectrum of this record (Figure 5b) shows concentrations of energy at periods of 41, 23, and 19 kyr (0.024, 0.043, and 0.053 cycles/kyr, respectively). Less energetic, but significant, peaks are also present near 100, 28, and 15 kyr (0.01, 0.036, 0.067 cycles/kyr, respectively). The bicoherence spectrum for this record (Figure 5c), shows that many modes in the radiative forcing are strongly coupled. Significant ($1-\alpha=0.90$) phase coupling between eccentricity and precession is indicated by $b(0.041, 0.012) = 0.978$ (region A in Figure 5c). The bicoherence spectrum also indicates significant coupling between orbital tilt and precession. For example, $b(0.041, 0.025) = 0.960$ (region B in Figure 5c) and $b(0.055, 0.023) = 0.969$ (region C in Figure 5c). The third components in these interacting triads have frequencies 0.066 (15 kyr) and 0.078 (12.8 kyr), respectively, and appear as less energetic peaks in the radiation power spectrum (Figure 5b).

The most notable interaction is at the triad (0.041, 0.012, 0.053), (region A in Figure 5c), which has a bicoherence of 0.978. This high value of bicoherence indicates that precession components of 19 and 23 kyr are nonlinearly coupled to 100 kyr eccentricity terms (although 0.012 cycles/kyr is a 83 kyr period, this frequency represents the 100 kyr band after averaging has been completed). This result is confirmed by examining the terms in the series expansion of eccentricity and precession given by Berger [1977, Tables 1 and 3]. Difference interactions between the individual precession terms listed in this reference can produce virtually all of the listed eccentricity

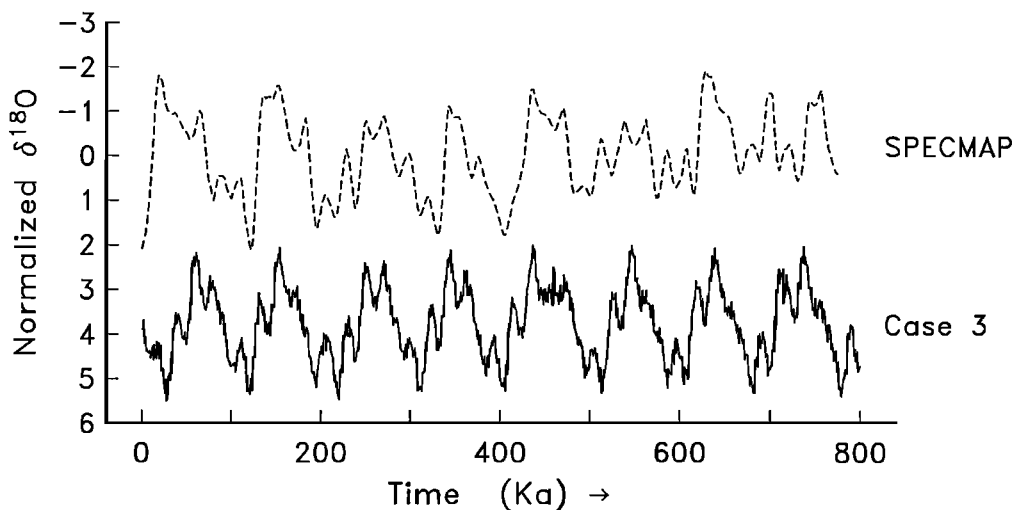


Fig. 4. SPECMAP composite $\delta^{18}\text{O}$ stack (dashed line) [Imbrie et al., 1984] compared to part of a modified version of case 3 (solid line) (see Figure 1c). The amplitude of f_1 is the same as in case 3, but the amplitudes of f_2 and f_3 have been reduced 60% and 70%, respectively.

terms [Berger, 1989]. This difference interaction indicates that at frequency $f_2 = 0.012$ cycles/kyr (100 kyr band), greater than 95% of the variance is quadratically coupled to oscillations at $f_1 = 0.41$ cycles/kyr (23 kyr) and $f_3 = 0.53$ cycles/kyr (19 kyr). The energy at 100 kyr is small in comparison with that at 41, 23, and 19 kyr (Figure 5b). However, almost all of the variance at 100 kyr is quadratically coupled through nonlinear interactions with the precessional terms. The biphasic of the (0.041, 0.012, 0.053) triad is zero, indicating that the phase of f_2 is equal to the difference of the phases of f_3 and f_1 . This is also confirmed by Berger [1977], as differences between the phases of the individual precession terms listed are exactly equal to the corresponding phases of the eccentricity terms.

In addition to significant bicoherence values, other analyses suggest that the observed phase couplings do not result from random fluctuations. Time series generated by replacing the

phases in the July 65°N radiation time series (Figure 5a) with random phases uniformly distributed over $(0, 2\pi)$ are shown in Figure 6a. The power spectrum of this random phase time series (Figure 6b) is identical to that of the radiation record (Figure 5b) because phase information is not retained by the power spectrum. The bicoherence spectrum (Figure 6c) of this random phase record clearly indicates an absence of phase coupling, as is expected for a purely linear system. Similar to case 1 above, the two values above the 0.90 significance level, $(0.039, 0.037, 0.076) = 0.509$ and $(0.105, 0.008, 0.113) = 0.589$, represent high bicoherence values that can be expected to occur through random chance. The result of the random phase simulation shown in Figure 6 is consistent with the conclusion that the high bicoherences observed in the radiation record are not a result of random fluctuations, but result from phase couplings within the orbital record. Similar low values

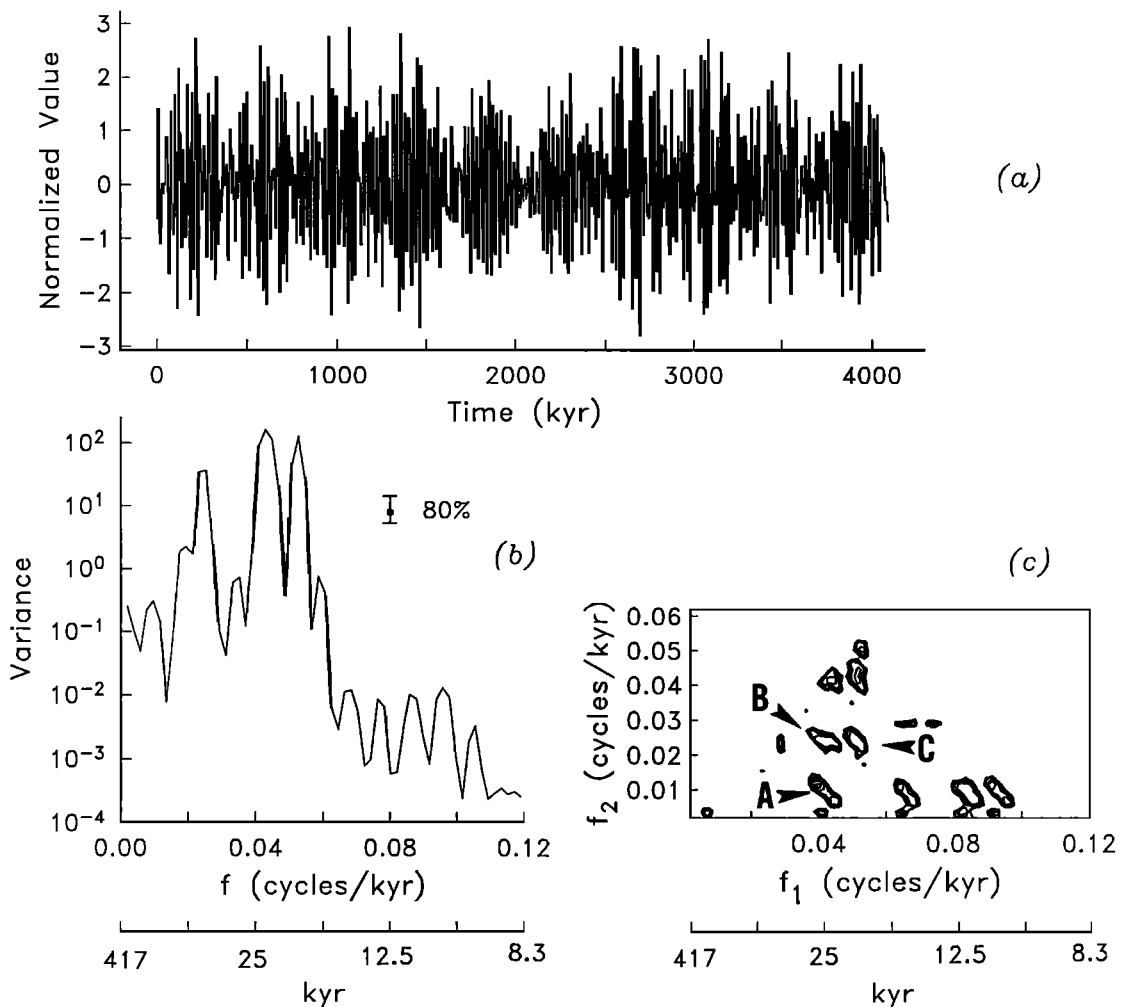


Fig. 5. July 65°N insolation, for the interval from 4.096 to 0 Ma (from Berger, [1978b] solution): (a) time series, (b) power spectra, and (c) significant ($1-\alpha = 0.90$) contours of bicoherence. The minimum value contoured is 0.57, and contour interval is 0.10. To obtain power spectral and bispectral estimates having 14 degrees of freedom, data were Hanning windowed, and eight ensembles of 0.512 m.y. length were averaged. Regions A, B, and C are referred to in the text.

of bicoherence were observed in several other random phase simulations (not shown).

These results illustrate the use of bispectral analyses for detecting quadratically nonlinear interactions. Strong nonlinear coupling is detected between oscillations in the precession and eccentricity bands in the estimated record of radiative forcing of Berger [1978b]. Using the terms given by Berger [1977], a difference interaction of precession terms is equivalent to eccentricity [Berger, 1989]. This interaction was not observable through examination of the time series and power spectra. The bicoherence spectrum also indicates significant nonlinear interactions between precession and obliquity. In the present solution of Berger [1978b], the strength of these nonlinear interactions does not vary through time, and thus analysis of a 4 m.y. record yields the same results as analysis of shorter (1 m.y.) records.

A purely linear response of climate to this nonlinear forcing will produce a paleoclimatic record that contains the same

nonlinear interactions as the forcing. The response will also be linearly coherent with the forcing at the forcing frequencies. On the other hand, a nonlinear response of climate to this nonlinear forcing will produce responses that are not necessarily coherent with oscillations at the same frequencies as the forcing. In the next section, three records of paleoclimate are examined to determine the extent of linear and nonlinear responses to orbital forcing.

ANALYSIS OF $\delta^{18}\text{O}$ RECORDS

The relatively short record lengths (typically 400-800 kyr) of most paleoclimatic time series has precluded application of bispectral analysis in the past. Variance of bispectral estimates are higher than power spectral estimates, and short records do not have enough degrees of freedom to yield statistically stable results. Recent efforts, however, have produced a number of long (>1 m.y.) records of paleoclimatic

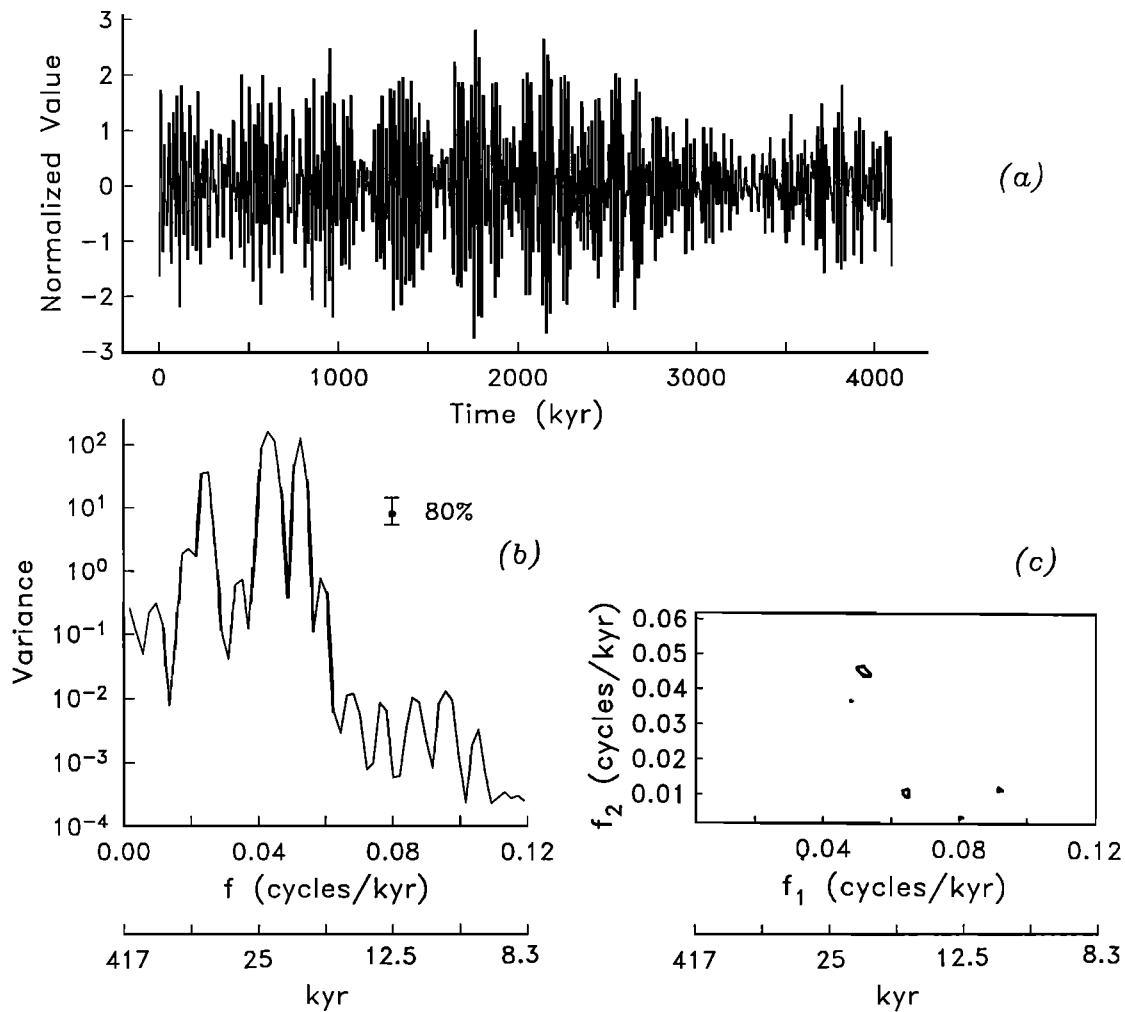


Fig. 6. Simulated time series generated by replacing the phases in the July 65°N insolation record (Figure 5a) with random phases. Power spectral and bispectral estimates were obtained as described in Figure 5: (a) time series, (b) power spectra, and (c) significant ($1-\alpha=0.90$) contours of bicoherence.

change [Shackleton and Hall, 1989; Ruddiman et al., 1989; Raymo et al., 1989]. The bispectrum of three relatively long $\delta^{18}\text{O}$ records from the North Atlantic and eastern equatorial Pacific are now examined.

The records examined here were taken from Ocean Drilling Project site 677 (eastern equatorial Pacific, $1^{\circ}12'\text{N}$, $83^{\circ}44'\text{W}$) and Deep Sea Drilling Project site 607 (North Atlantic, $41^{\circ}00'\text{N}$, $32^{\circ}58'\text{W}$). At site 677, time series of planktic and benthic $\delta^{18}\text{O}$ were examined, and at site 607, benthic $\delta^{18}\text{O}$ time series were examined. The site 677 record was generated and initially studied by Shackleton and Hall [1989] and Shackleton et al. [1990]. The site 607 record was generated and studied by Ruddiman et al. [1989] and Raymo et al. [1989]. For each of these studies the authors have developed a chronology for these records by making use of orbital tuning procedures. Differences between the time scale used by Shackleton et al. [1990] and Ruddiman et al. [1989] and Raymo et al. [1989] are substantial. The issue of chronologies and approaches to orbital tuning is complicated, and for consistency, only the most recent time scale of Shackleton et al. [1990] is used here. This time scale has been applied to both the 677 and 607 records [Shackleton et al., 1990]. Although it appears that the site 677 and site 607 bispectra presented here are robust to slight time scale changes, the potentially critical effects of time scale variability on bispectrum estimates will be treated in a later paper.

The time series of planktic (*Globorignoides ruber*) and benthic (primarily *Uvigerina senticosus*) $\delta^{18}\text{O}$ from site 677, and benthic (*Cibicidoides*) $\delta^{18}\text{O}$ from site 607 are shown in Figure 7. The records from site 677 are approximately 2.6 m.y. in length, while the site 607 record is approximately 2.8 m.y. long. The average sampling interval for the 677 data is 2000 years, and the average for the 607 data is 3500 years.

It is well known that a change in the character of the Neogene global ice volume record occurred near 1 Ma [Pisias and Moore, 1981; Ruddiman and Raymo, 1988]. Oscillations at around 100 kyr, which are generally not prevalent previous to 1 Ma, become very strong in the late Pleistocene. This is clearly seen by comparing the power spectra of these records before (Figure 8a) and after (Figure 8b) 1 Ma. Because of this

apparent nonstationarity in the record, all records are analyzed in two parts, from 1.0 to 0 Ma and from 2.6 to 1.0 Ma (2.8 to 1.0 Ma at site 607). The records are divided at 1.0 Ma to obtain the longest late Pleistocene record possible. The precise location (within ± 100 kyr) where the records are divided does not change the results significantly.

So that each $\delta^{18}\text{O}$ time series could be processed identically, the time series from site 607 was overinterpolated to match the sampling resolution of the site 677 data. While the Nyquist frequency of the 607 time series is at 7 kyr (as opposed to 4 kyr in the case of the site 677 records), this oversampling allows for direct comparison of the three data sets after processing. For the interval from 1.0 to 0 Ma, all smoothed spectral estimates were obtained by averaging four 128 point (256 kyr) ensembles for 6 degrees of freedom. For the interval from 2.6 to 1.0 Ma, smoothed estimates were obtained by averaging six 128-point ensembles for 10 degrees of freedom. In each case the frequency resolution is 0.0039 cycles/kyr, and a Hanning window was used to reduce leakage. (Results using this method of spectral analysis were not significantly different than results obtained using the Blackman-Tukey truncated lag (autocovariance) method.)

For the interval from 1.0 to 0 Ma, the power spectrum of each $\delta^{18}\text{O}$ record has variance concentrated at the Milankovitch frequencies of 0.012, 0.023, 0.043, and 0.053 cycles/kyr, corresponding to the 100, 41, and 23, and 19 kyr bands, respectively (Figure 8a). While the site 677 records show significant variance concentrated at the precessional frequency of 19 kyr, this peak is not prominent in the site 607 data. The planktic $\delta^{18}\text{O}$ time series for site 677 contains additional variance at periods of 15 kyr and 12 kyr, which correspond to sum frequencies of orbital precession and obliquity, and the site 607 time series contains significant variance near 15 kyr as well.

For the interval from 2.6 to 1.0 Ma, the total variance contained in each time series is lower than in the interval from 1.0 to 0 Ma. Each time series shows variance concentrated primarily at 41 kyr (0.023 cycles/kyr) (Figure 8b). Low-frequency power, dominant from 1.0 to 0 Ma, is diminished relative to 41 kyr power. In each time series, low-frequency

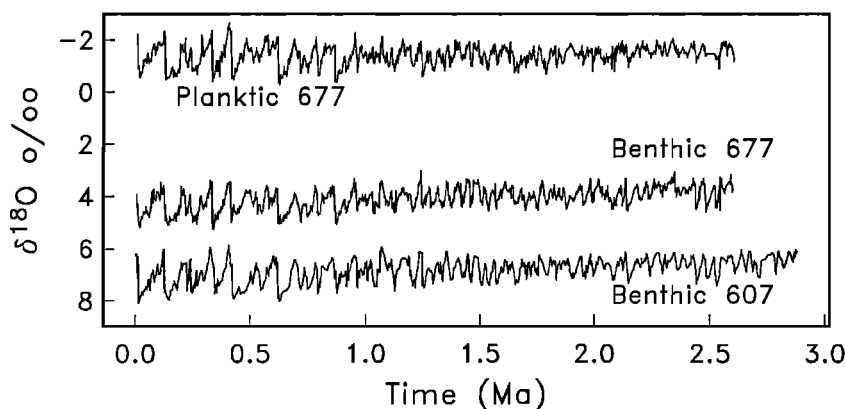


Fig. 7. Time series of planktic (*G. ruber*) and benthic (primarily *Uvigerina*) $\delta^{18}\text{O}$ from site 677 [Shackleton and Hall, 1989] and benthic (*Cibicidoides*) $\delta^{18}\text{O}$ from site 607 [Ruddiman et al., 1989; Raymo et al., 1989]. The 607 data are offset from actual values to allow visual comparison.

variance is distributed between 400 kyr and 71 kyr, rather than concentrated at 100 kyr. In this older interval, the site 677 planktic $\delta^{18}\text{O}$ record also shows power at 23 kyr. This 23 kyr peak is also present in the benthic records, although to a lesser extent than in the site 677 planktic $\delta^{18}\text{O}$.

Coherence and phase spectra between July 65°N insolation and each $\delta^{18}\text{O}$ time series for 1.0 to 0 Ma and from 2.6 to 1.0 Ma are displayed in Figures 9 and 10 and are summarized in Table 1. In the interval from 1.0 to 0 Ma, significant ($1-\alpha = 0.90$) coherence occurs at the four primary Milankovitch frequencies for each time series. The coherence spectrum at site 607 is similar to that of both site 677 records, although coherence with insolation at 23 kyr is weaker, and coherency at 100 kyr occurs over a wider band. With the exception of the 41 kyr band in the insolation/site 607 phase spectrum, the phase spectrum for each record is similar. As noted in the Introduction, this overall high coherence between insolation and $\delta^{18}\text{O}$ provides evidence for a strong linear relationship between insolation forcing and the paleoclimatic response.

Coherence with insolation is weaker in the interval from 2.6 to 1.0 Ma. Significant coherence with insolation occurs in the

41 kyr and 23 kyr bands with each isotopic time series, and in the 19 kyr band in the site 677 time series (Figure 10 and Table 1). The coherence is not as strong as in the interval from 1.0 to 0 Ma, however. In each time series, there is significant coherence with insolation at frequencies lower than 100 kyr. In addition, the site 607 time series shows high coherence with insolation near 30 kyr. In this time interval, each of the insolation/ $\delta^{18}\text{O}$ phase spectra are similar.

Returning to the 1.0 to 0 Ma records, coherence between insolation and $\delta^{18}\text{O}$ near 100 cycles/kyr is estimated as 0.91, 0.79, and 0.89 for the 677 planktic, 677 benthic, and 607 benthic records, respectively. If these estimates represent the true value of coherence (these estimates are not corrected for a small bias), then between 62% and 82% of the variance in the $\delta^{18}\text{O}$ record is linearly related to variations in direct eccentricity forcing. For 677 planktic and benthic data, the phase of the response changes by close to 90° near 100 kyr, and for each record the gain at 100 kyr is relatively high (Table 1). These results are consistent with a response at 100 kyr which is linear and resonant. This is discussed below.

The bicoherence spectra for each $\delta^{18}\text{O}$ record over the 1.0 to

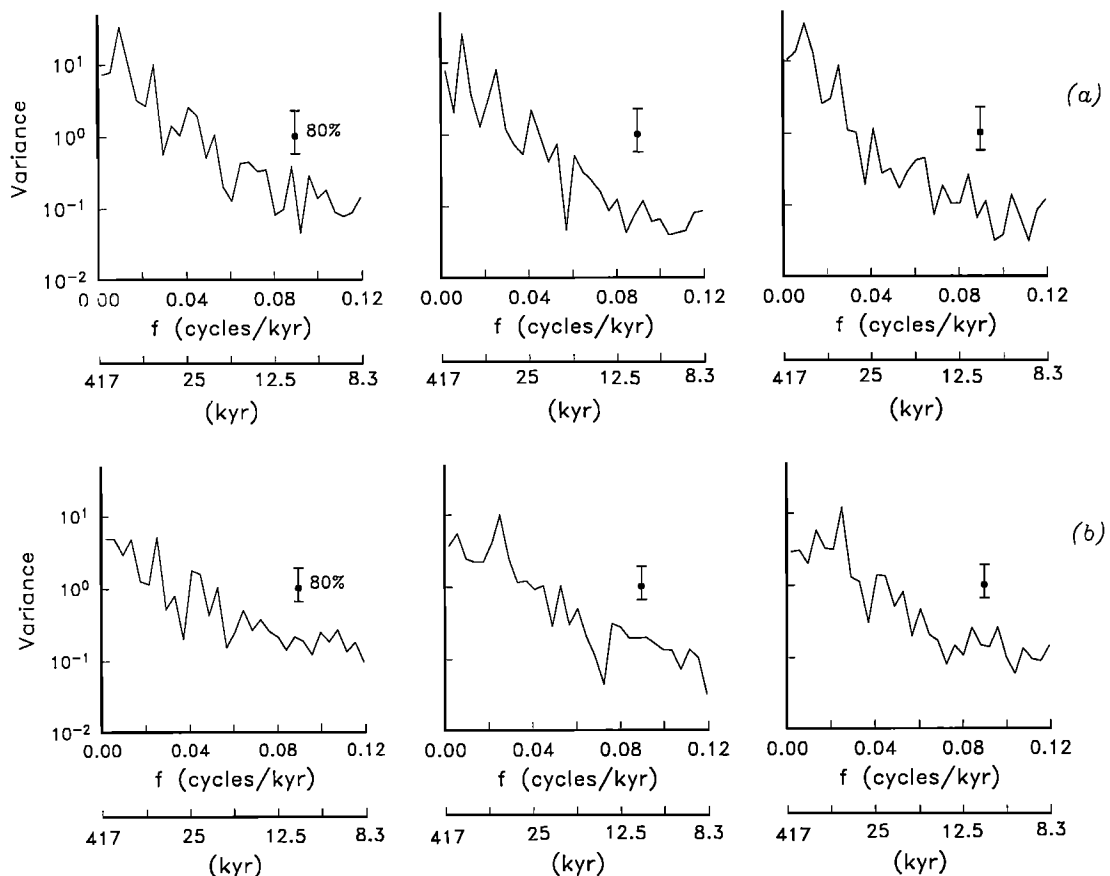


Fig. 8. (a) Power spectra of isotopic records for the interval 1.0 to 0 Ma: site 677 planktic $\delta^{18}\text{O}$ (left), site 677 benthic $\delta^{18}\text{O}$ (middle), and site 607 benthic $\delta^{18}\text{O}$ (right). Estimates having 6 degrees of freedom were obtained by using a Hanning window and averaging four 256 kyr subrecords. (b) Power spectra for the interval 2.6 to 1.0 Ma: site 677 planktic $\delta^{18}\text{O}$ (left), site 677 benthic $\delta^{18}\text{O}$ (middle), and site 607 benthic $\delta^{18}\text{O}$ (right). Estimates having 10 degrees of freedom were obtained using a Hanning window and averaging six 256 kyr subrecords.

0 Ma interval are shown in Figures 11a-11c. Smoothed bispectral estimates were calculated in the same manner as the corresponding power spectral and cross-spectral estimates. Bispectra calculated from short records have coarser frequency resolution, as is clearly illustrated in Figure 11d, where the bicoherence spectrum of 65°N insolation for a 1 m.y. record is

shown (compare to Figure 5c, the bicoherence spectrum for a 4.096 m.y. record). The estimates for the 4 m.y. record shown in Figure 5c have 14 dof, and the 0.90 significance level is 0.58. The 1 m.y. record (Figure 11d), on the other hand, has 6 dof, and the 0.90 significance level is 0.88 (bicoherences reported below are significant at a 0.80 level). Owing to the

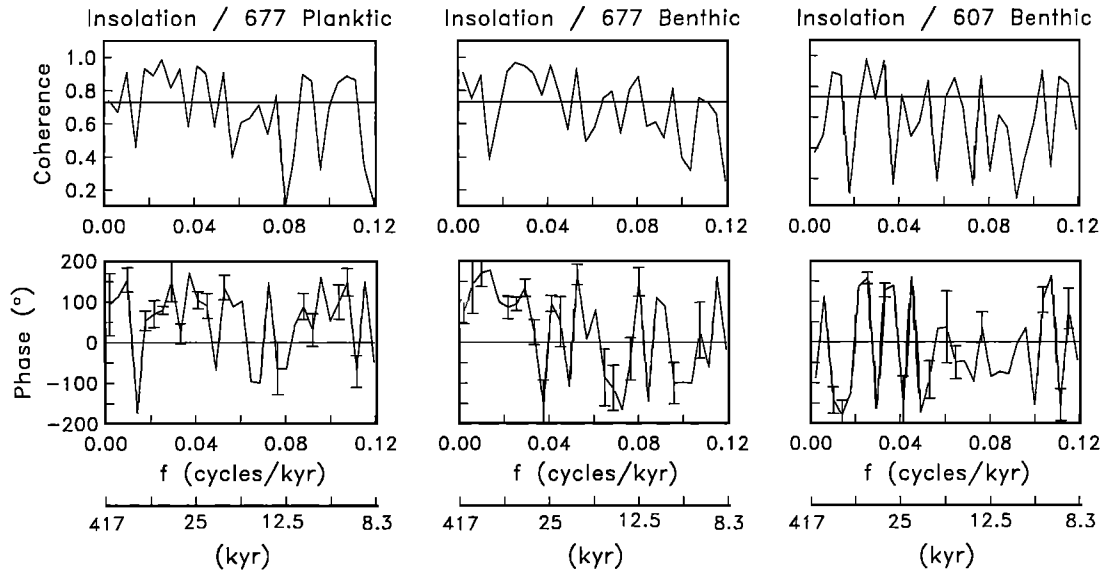


Fig. 9. Coherence (top) and phase (bottom) between 65°N insolation and $\delta^{18}\text{O}$, for the interval from 1.0 to 0 Ma: site 677 planktic $\delta^{18}\text{O}$ (left), 677 benthic $\delta^{18}\text{O}$ (middle), and site 607 benthic $\delta^{18}\text{O}$ (right). The 90% significance level for coherence (horizontal line) is 0.73. The 90% confidence interval for phase estimates is indicated by vertical bars. Positive phase indicates insolation leads $\delta^{18}\text{O}$. The data were processed as described in the caption to Figure 8a.

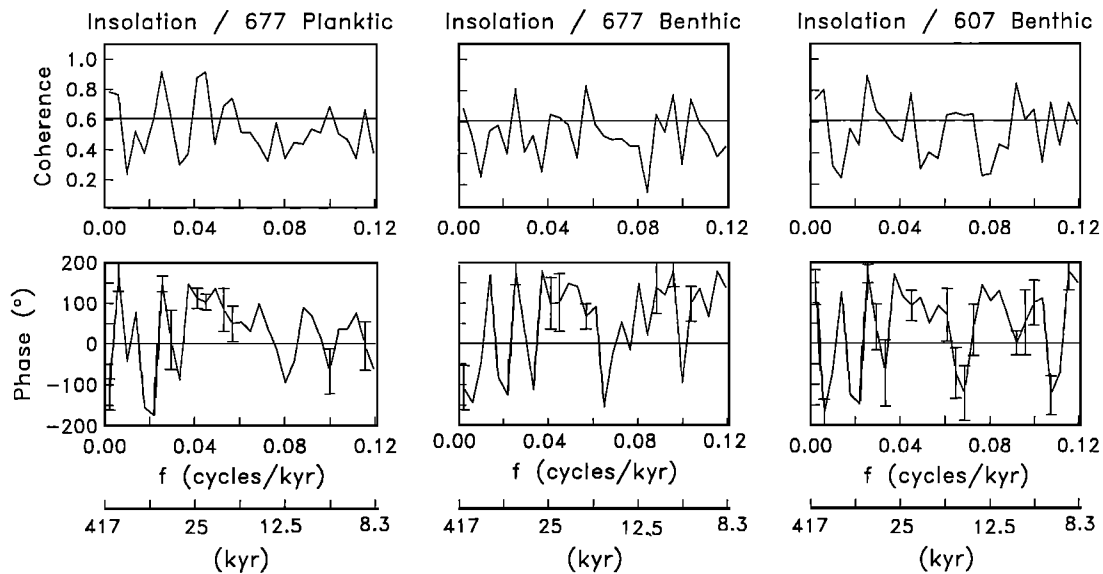


Fig. 10. Coherence (top) and phase (bottom) between 65°N insolation and $\delta^{18}\text{O}$, for the interval from 2.6 to 1.0 Ma: site 677 planktic $\delta^{18}\text{O}$ (left), 677 benthic $\delta^{18}\text{O}$ (middle), and site 607 benthic $\delta^{18}\text{O}$ (right). The 90% significance level for coherence (horizontal line) is 0.61. The 90% confidence interval for phase estimates is indicated by vertical bars. Positive phase indicates insolation leads $\delta^{18}\text{O}$. The data were processed as described in the caption to Figure 8b.

low degrees of freedom for these time series, the bias of the observed bicoherences is not negligible [Elgar and Sebert, 1989]. Although the bicoherence values reported in this section have not been corrected for bias, such a correction would not significantly change the overall results presented here.

For the interval from 1.0 to 0 Ma at site 677, statistically significant ($1-\alpha=0.80$) bicoherences indicate phase coupling among components which are also coupled in the insolation record, as well as among components which are not coupled in the insolation record. In both the planktic and benthic $\delta^{18}\text{O}$ records, phase coupling occurs between oscillations at 0.012 cycles/kyr (100 kyr band), 0.043 cycles/kyr (23 kyr band), and 0.053 cycles/kyr (19 kyr band). For the planktic record, $b(0.043, 0.012) = 0.794$, and for the benthic record, $b(0.043, 0.012) = 0.792$. The phase relationship between these modes has changed, however, from a biphasic of 0° in the insolation forcing to a biphasic of -90° in the benthic data and -114° in the planktic data (these biphasic values of -90° and -114° are within

an 80% confidence interval of one other and thus are not statistically different). There are also statistically significant couplings in the site 677 records between 23 kyr band variations and 41 kyr ($b(0.043, 0.023)=0.840$ in the planktic record and $b(0.043, 0.023) = 0.741$ in the benthic record).

This phase coupling, also present in the insolation forcing, indicates that oscillations at periods of 23 kyr and 41 kyr are coupled to oscillations at 15 kyr. Finally, statistically significant phase coupling is present between 41, 100, and 30 kyr oscillations ($b(0.023, 0.012) = 0.723$ in the planktic record and $b(0.023, 0.012) = 0.772$ in the benthic record). This last interaction is not present in the insolation forcing and could represent part of a nonlinear response in the climate system.

The bispectrum for site 607 is different than that for site 677 from 1.0 to 0 Ma. Statistically significant phase coupling occurs among two triads of frequencies, (0.051, 0.016, 0.067) and (0.051, 0.043, 0.094), with bicoherences of 0.520 and 0.766, respectively. While the latter triad is also present in the insolation bispectrum, this phase coupling involves higher

TABLE 1. Coherence, Gain, and Phase Shift Between Insolation and $\delta^{18}\text{O}$ Response Near 100, 41, 23, and 19 kyr Periods for the Intervals from 1.0 to 0 and from 2.6 to 1.0 Ma

Record	Frequency, cycles/kyr	Period, kyr	Coherency	Gain	Phase, deg
<i>0-1 Ma</i>					
677 planktic	0.012	~100	0.9076	9.220	154
	0.023	~ 41	0.9877	0.488	79
	0.043	~ 23	0.9504	0.134	105
	0.053	~ 19	0.9077	0.087	136
677 benthic	0.012	~100	0.7903	7.739	170
	0.023	~ 41	0.9677	0.429	95
	0.043	~ 23	0.9529	0.124	96
	0.053	~ 19	0.9301	0.074	167
607 benthic	0.012	~100	0.8948	9.096	-142
	0.023	~ 41	0.9755	0.448	158
	0.043	~ 23	0.7437	0.070	75
	0.053	~ 19	0.8320	0.032	-92
<i>1-2.6 Ma</i>					
677 planktic	0.0101	~100	0.2409	1.221	-40
	0.0257	~ 41	0.9181	0.342	148
	0.0452	~ 23	0.9141	0.096	103
	0.0570	~ 19	0.7407	0.055	5
677 benthic	0.0101	~100	0.2493	1.154	-48
	0.0257	~ 41	0.8065	0.415	179
	0.0452	~ 23	0.6275	0.053	101
	0.0570	~ 19	0.8283	0.859	67
607 benthic	0.0101	~100	0.3197	1.334	-63
	0.0257	~ 41	0.8949	0.508	171
	0.0452	~ 23	0.7807	0.074	93
	0.0570	~ 19	0.3658	0.309	-93

frequencies that are close to the Nyquist frequency for this time series. With this time series, it is particularly notable that no significant phase coupling occurs with oscillations at 41 kyr or 100 kyr, as in the site 677 records. For instance, while power spectral peaks are present at 100, 41, and 15 kyr in the site 607 data, the bicoherence for this triad is not significant at

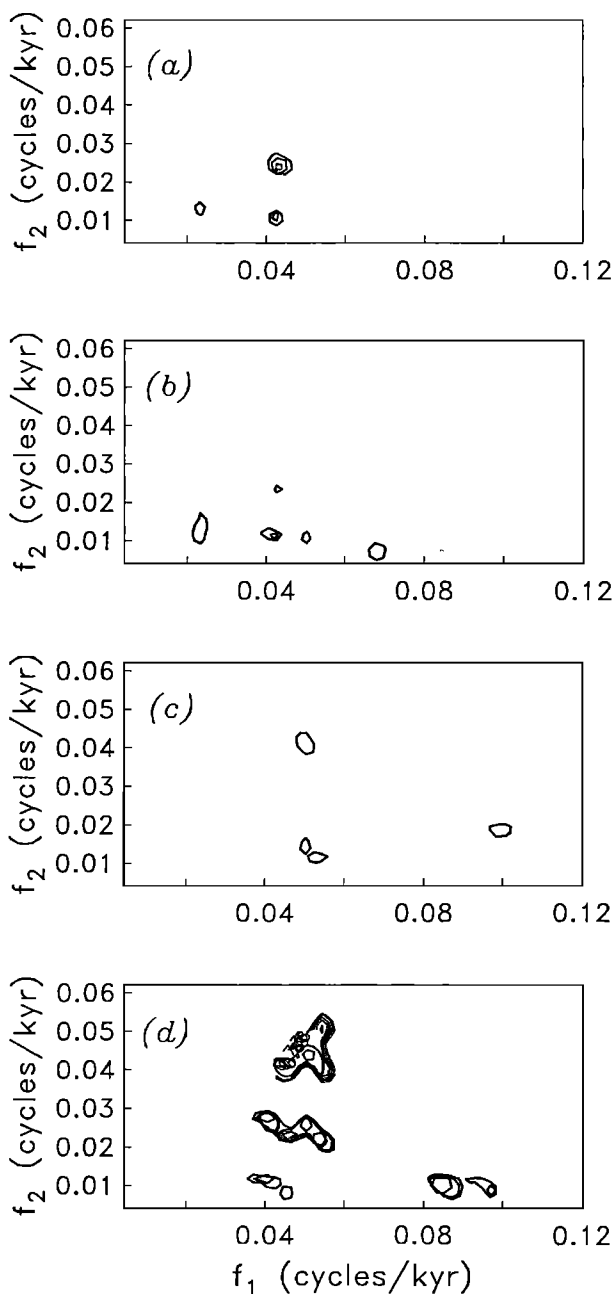


Fig. 11. Contours of bicoherence, for the interval from 1.0 to 0 Ma. The data were processed as described in the caption to Figure 8a. The minimum bicoherence value contoured (significant at a 80% level) is 0.73 with a contour interval of 0.05: (a) site 677 planktic $\delta^{18}\text{O}$, (b) site 677 benthic $\delta^{18}\text{O}$, (c) site 607 benthic $\delta^{18}\text{O}$, and (d) 65°N insolation.

a 0.80 level. In the site 677 data, on the other hand, the bicoherence for this triad is statistically significant. While the cause of this discrepancy between Atlantic and Pacific $\delta^{18}\text{O}$ data sets warrants further study, the low bicoherences in the site 607 data may be an artifact of the low degrees of freedom.

At site 677, evidence for a nonlinear response of the climate system to orbital forcing is given by high bicoherence in the (0.023, 0.012, 0.035) triad. However, the results at site 677 are also noteworthy because of the similarity of the phase couplings in the climate response to those in the orbital forcing. The phase coupled oscillations present in $\delta^{18}\text{O}$ time series from this site includes several of the same modes that are coupled in the forcing. This is consistent with a linear response of the climate system to insolation forcing. Changes in the phase relationships between each mode occur, however, because the biphasers for every coupled triad in the data are close to -90° , whereas in the insolation record the corresponding biphasers are near 0° .

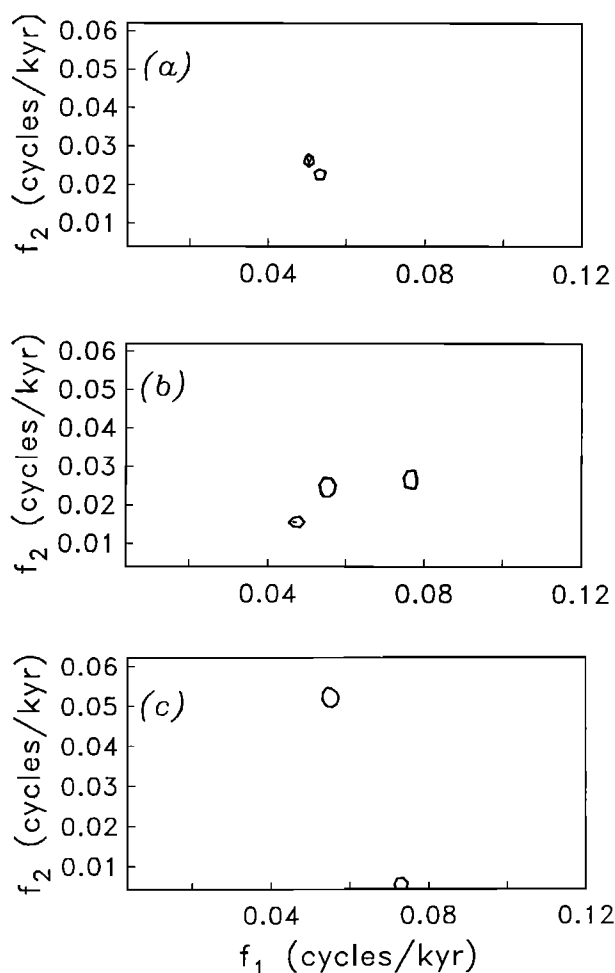


Fig. 12. Contours of bicoherence, for the interval from 2.6 to 1.0 Ma. The data were processed as described in the caption to Figure 8b. The minimum bicoherence value contoured (significant at a 80% level) is 0.57 with a contour interval of 0.05: (a) site 677 planktic $\delta^{18}\text{O}$, (b) site 677 benthic $\delta^{18}\text{O}$, and (c) site 607 benthic $\delta^{18}\text{O}$.

As with the radiation time series above, simulations with synthetic time series can be used to reinforce these results. Synthetic time series were generated for the site 677 and site 607 $\delta^{18}\text{O}$ data over the 1.0 to 0 Ma time interval. The amplitude spectrum of each time series was preserved, but the observed phases were replaced with random phases. For each record, 10 simulations were made, and the bispectrum calculated for each. At site 677, although some significant bicoherences occurred in the planktic data (through random chance, expected at an 80% level), no simulation showed significant bicoherence at the same sets of triads that are coupled in the insolation forcing. For the site 677 benthic data, bicoherences from only one in 10 simulations resemble those in the insolation data. At site 607, significant bicoherences similar to the data occur in two simulations, consistent with an 80% significance level. These results add strength to the argument that despite the low degrees of freedom of these records, the couplings observed in the data are indeed significant and are not likely to be caused by random fluctuations.

Bicoherences for the site 677 and 607 $\delta^{18}\text{O}$ time series for the interval from 2.6 to 1.0 Ma are shown in Figure 12. Bicoherences from the site 677 planktic $\delta^{18}\text{O}$ data show one region of statistically significant ($1-\alpha = 0.80$) phase coupling that is similar to the insolation forcing (the triad consisting of oscillations at 19, 41, and 12 kyr has $b=0.662$). This same phase coupling is present in the site 677 benthic $\delta^{18}\text{O}$, where $b=0.603$. In the benthic 677 data, two other triads have significant bicoherences that are not similar to coupled modes in the insolation forcing, $b(0.047, 0.016) = 0.620$ and $b(0.078, 0.027) = 0.606$. At site 607, the only significant phase coupling occurs among high-frequency components ($b(0.055, 0.051) = 0.599$).

Unlike the interval from 1.0 to 0 Ma, the results from the lower Pleistocene and upper Pliocene $\delta^{18}\text{O}$ time series do not strongly support a linear response of the paleoclimate record to insolation forcing. Only one coupled triad that is present in the insolation record has high bicoherence in the site 677 records. Orbital frequencies that contain most of the variance in the $\delta^{18}\text{O}$ power spectrum for 2.6 to 1.0 Ma do not appear to be as strongly coupled to insolation as in the 1.0 to 0 Ma interval. Oscillations having a 62-70 kyr period, present in the $\delta^{18}\text{O}$ power spectra for 2.6 to 1.0 Ma, are phase coupled to 19 kyr oscillations in the site 677 benthic $\delta^{18}\text{O}$ data. As there is no coherence between insolation and $\delta^{18}\text{O}$ at this frequency (Figure 10), the 62-70 kyr peak may represent a nonlinear (difference interaction) between 15 kyr and 19 kyr. Together, these observations indicate a change in the nature of the climate response between 1.0 to 0 Ma and 2.6 to 1.0 Ma.

Similar to the results for the 1.0 to 0 Ma interval, numerical simulations with synthetic time series having random phases suggest that the observed bicoherences (Figure 12) were not caused by random fluctuations. At site 677 for both planktic and benthic $\delta^{18}\text{O}$ data, bicoherences of the simulated, random phase records were similar to bicoherences of the data in only 2 of 10 simulations. At site 607, only one simulation had phase coupling similar to that observed in the data. In no case did the significant bicoherences resemble those of the insolation data. Thus, as in the 1.0 to 0 Ma interval, these simulations add supporting evidence that the phase couplings suggested by bispectral analysis are not due to random fluctuations.

In summary, bispectral estimates for site 677 $\delta^{18}\text{O}$ data indicate that from 1.0 to 0 Ma, phase couplings similar to those present in the insolation time series occur. This is consistent with a linear response to insolation forcing. This result is not seen in the 1.0 to 0 Ma benthic $\delta^{18}\text{O}$ time series from site 607, however. From 2.6 to 1.0 Ma, evidence for a linear response of the $\delta^{18}\text{O}$ record is not as strong at either location. Although all of the time series have very low numbers of degrees of freedom, and correspondingly high nonzero significance levels, Monte Carlo simulations suggest that the significant bicoherences observed are not caused by random fluctuations.

EVOLUTION OF THIRD MOMENTS

As noted above, the "mid-Pleistocene transition" of global $\delta^{18}\text{O}$ records from a mainly 41 kyr oscillation in the early Pleistocene to a 100 kyr "sawtooth" shape oscillation in the late Pleistocene is well known. Subsequent models of paleoclimate have sought to reproduce this asymmetric response [Saltzman and Maasch, 1988]. The evolution of skewness and asymmetry (normalized third moments, as defined above) of the site 677 and site 607 $\delta^{18}\text{O}$ time series are now examined. These third-moment quantities are related to the shape of the time series (as shown in the example above) and are given by the integrated real and imaginary parts of the bispectrum, respectively [Elgar and Guza, 1985; Elgar, 1987]. The third moments allow the observed long-term evolution of the $\delta^{18}\text{O}$ record to be quantified.

The evolution of the skewness and asymmetry of the site 607 and site 677 $\delta^{18}\text{O}$ records is shown in Figure 13. Skewness and asymmetry are calculated for overlapping 512-point records, that is, from 1.0 to 0 Ma, from 1.5 to 0.5 Ma, from 2.0 to 1.0 Ma, and from 2.5 to 1.5 Ma (because it is 2.8 m.y. long, for site 607 estimates from 2.8 to 1.8 Ma are included). There is an increase in the asymmetry (sawtoothness) of the time series from 2.5 Ma to present and a simultaneous decrease in the skewness (peakedness) of the record. In the oldest part of the records, there is relatively high skewness which decreases to near zero in the late Pleistocene. Monte Carlo simulations suggest that these third-moment estimates are significantly different from zero. (Recall that for no coupling (a Gaussian time series) the third moments are zero.)

There are large differences between the skewness and asymmetry of the $\delta^{18}\text{O}$ records and that of the insolation record (Figure 14). The asymmetry of the insolation record is close to zero throughout the past 2.5 m.y., and skewness is only slightly greater than zero. Thus, although the climate system is responding linearly to insolation forcing (at least over the last million years), the nature of the phase coupling within the system is evolving. This observation is consistent with the results of Pisias et al. [1990], who showed evidence for a nonconstant phase between orbital forcing and ice volume over the past 700,000 years.

DISCUSSION

The analyses above demonstrate that the orbital parameters which combine to cause long-term changes in solar insolation are nonlinearly coupled to one another. In particular, the coupling between precession terms of 23 kyr and 19 kyr and

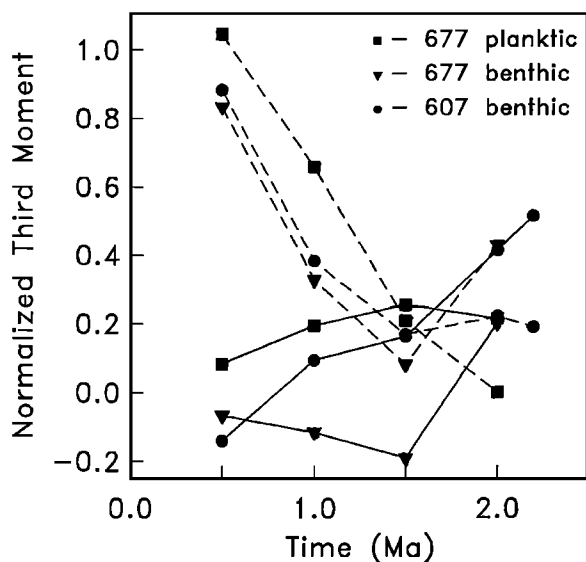


Fig. 13. Skewness (solid line) and asymmetry (dashed line) of $\delta^{18}\text{O}$ records versus time. Each symbol represents a 1 m.y. average and is plotted at the midpoint of the time interval. Squares indicate 677 planktic $\delta^{18}\text{O}$; triangles, 677 benthic $\delta^{18}\text{O}$; and circles, 607 benthic $\delta^{18}\text{O}$.

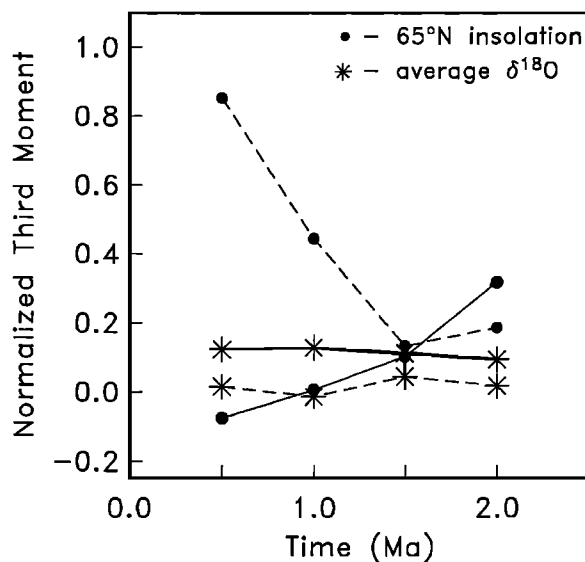


Fig. 14. Skewness (solid line) and asymmetry (dashed line) of the average of the three $\delta^{18}\text{O}$ records presented in Figure 13 (circles), and skewness and asymmetry of 65°N insolation (asterisks) versus time.

the 100 kyr eccentricity parameter is very strong. With respect to this coupling, it is important to note that the strength of the precession-eccentricity coupling in the insolation forcing is related to the presence of the $1/(1-e^2)$ term in the insolation formula used in this study. Only the solution of Berger [1978b] includes this term. Previous insolation solutions have not included it [see Berger, 1978a] because it does not contribute significantly to the overall insolation change (around 0.1%). When this term is removed from the insolation formulae of Berger [1978b], the phase coupling between precession and eccentricity is weaker. Recalling that the only orbital element that can modify the total solar energy received by the Earth is eccentricity (although forcing at 100 kyr is small in comparison with precessional or obliquity forcing), this term is very important, as emphasized by Berger [1978a] and Berger [1989].

The dilemma of whether the 100 kyr peak present in the $\delta^{18}\text{O}$ spectrum during the late Pleistocene is a linear response to eccentricity forcing, or a nonlinear response to precession band interactions is now addressed. The insolation data indicate that eccentricity and precession bands are highly coupled in the insolation record. The linear coherence between insolation and $\delta^{18}\text{O}$ in the eccentricity band is greater than 0.90, and the same phase couplings are present in the isotopic record. These results suggest that a nonlinear response is not required to explain the observed response. A simple linear resonance model may help to explain the processes leading to the dominance of 100 kyr oscillations in the late Pleistocene ice volume record.

A brief review of resonance demonstrates that the results reported here are consistent with a resonant response to insolation forcing in the 100 kyr band. The simple physical system of a forced oscillator with damping is

$$x = \frac{F}{m(\omega_0^2 - \omega^2 + i\gamma\omega)} \quad (4)$$

where x is the displacement (i.e., response), F is the force driving the oscillator, m is the mass of the oscillator, ω_0 is the natural (resonant) frequency of the system, ω is the frequency of the forcing, and γ is the damping force. For the case of zero damping, the magnitude of x is related to the size of the force by the factor $1/(\omega_0^2 - \omega^2)$, and as ω approaches ω_0 , this magnitude approaches infinity. In this context, the gain of the system response is

$$\rho^2 = \frac{1}{m^2 [(\omega^2 - \omega_0^2)^2 + \gamma^2 \omega^2]} \quad (5)$$

The corresponding phase shift of the system response is given by

$$\theta = \arctan \left(-\frac{\gamma\omega}{\omega_0^2 - \omega^2} \right) \quad (6)$$

The gain and phase change of the system response for different values of ω are shown in Figure 15.

For any amount of damping (γ), maximum gain occurs where ω equals ω_0 . In addition, a phase change of up to 180° occurs as ω changes from $\omega > \omega_0$ to $\omega < \omega_0$. If solar insolation is the forcing, and the climate system response is being measured, then as a small amount of insolation is applied to this system at $\omega = 0.01$, the climate system response becomes greatly amplified because of the proximity of ω to ω_0 , the natural resonant frequency of the climate system.

The gain of the 100 kyr band in the insolation - $\delta^{18}\text{O}$ cross spectra is about an order of magnitude higher than the gain in

the 41 kyr band, and about 2 orders of magnitude higher than the gain in the 23, or 19 kyr bands (Figure 15 and Table 1). In addition, the phase spectra (Figures 9a and 16) show evidence for a shift which corresponds to that predicted by linear resonance. Note, however, that in this study July 65°N insolation values are used, and the phase of the response in the precession band depends on the particular month chosen. The

small amount of eccentricity forcing at 100 kyr (approximately 0.1% of the total variance in the insolation and approximately 3 orders of magnitude less than the variance of precessional forcing) may occur at or near a resonant frequency in the climatic system, and the large amplitude response observed in the $\delta^{18}\text{O}$ record results from this resonance. The absence of such a resonant response in the late Pliocene and lower

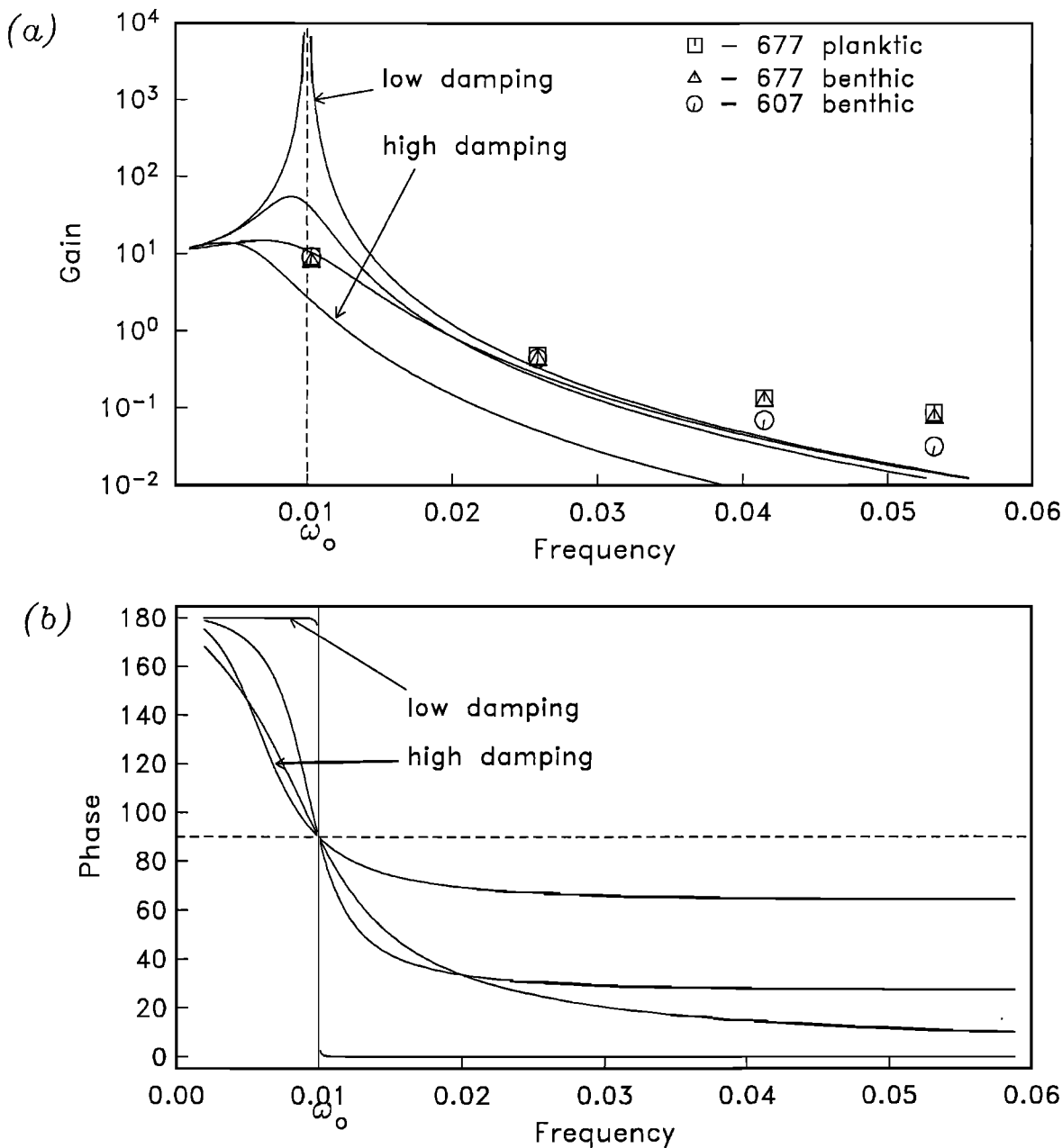


Fig. 15. (a) Gain versus frequency for the resonance model described in the text (equation (4)). Solid curves indicate the gain of the system response for different values of damping, γ . The vertical dashed line at ω_0 represents the resonant frequency of the system. Symbols plotted are the estimated gain of $\delta^{18}\text{O}$ from Table 1. Squares indicate 677 planktic $\delta^{18}\text{O}$; triangles, 677 benthic $\delta^{18}\text{O}$; and circles, 607 benthic $\delta^{18}\text{O}$. (b) Phase versus frequency for the resonance model described in the text (equation (4)).

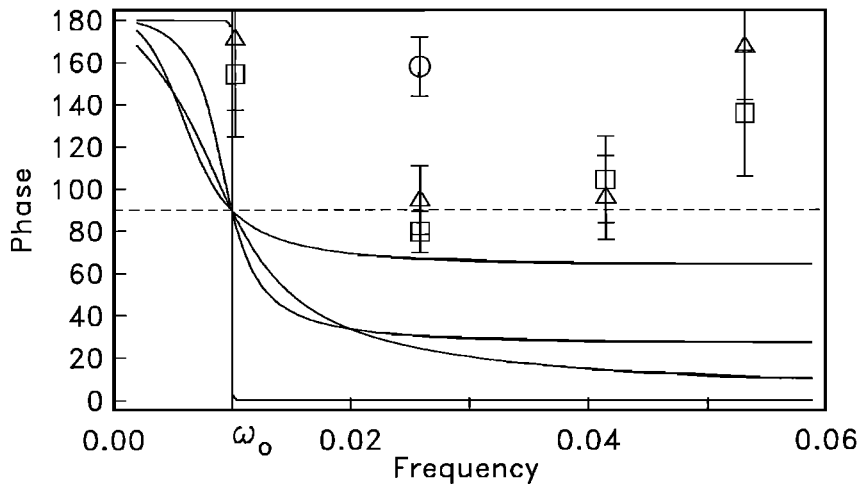


Fig. 16. Phase shift versus frequency for the resonance model described in the text (equation (4) and Figure 15b), compared to $\delta^{18}\text{O}$ phase from Table 1. The model phases have been shifted by 65° to allow comparison of the model to the data. Symbols plotted are the estimated phase of $\delta^{18}\text{O}$ from Table 1. Squares indicate 677 planktic $\delta^{18}\text{O}$; triangles, 677 benthic $\delta^{18}\text{O}$; and circles, 607 benthic $\delta^{18}\text{O}$. Vertical bars indicate 90% confidence intervals for the phase estimates.

Pleistocene may signify a changing resonant frequency as the climate system evolves.

Linear resonance is a straightforward method of accounting for the observed climate response of the past 1 m.y. As noted in the Introduction, paleoclimate models have explored a variety of mechanisms accounting for this climatic response. The observations presented here support the results of Saltzman and Sutera [1984] and Saltzman et al. [1984] that imply an inherently sensitive climate system at the 100 kyr period during the late Pleistocene. The observations also supports Berger's [1989] statement that the influence of eccentricity forcing alone is very important. While it is likely that a range of mechanisms, both linear and nonlinear, are acting to produce the observed climate response, the data presented here are consistent with a resonant response. Models which simulate climatic changes must be consistent with these observations.

This analysis has also demonstrated differences between the climatic response in the late Pleistocene, which may be primarily a linear response to insolation forcing, and the early Pleistocene/Pliocene, which may include a nonlinear response. The observations, including the evolution of third moments, suggest there is an evolution in the climatic response.

Finally, it is necessary to consider these results in light of some important assumptions that have been made to carry out the above analysis. It has been assumed that a correct time scale has been used. While it is known that different time scales will produce different results, it is unknown how sensitive bispectral estimates are to errors in the time scale. It has also been assumed that the above results are not an artifact of the particular orbital tuning strategy used by Shackleton et al. [1990]. This important issue is left to a separate study.

CONCLUSIONS

Bispectral analysis was used to detect nonlinear phase couplings in the time series of long-term solar insolation. Orbital eccentricity and precession are highly nonlinearly

coupled, as are precession and obliquity. The quadratic phase couplings present in the insolation forcing have been compared to phase couplings in the climatic time series of $\delta^{18}\text{O}$, a global ice volume proxy. Power spectra, cross spectra, and third moments (skewness and asymmetry) of the data suggest an evolution in the climate system response from late Pliocene to late Pleistocene. Quantitative estimates of this evolution are seen in increasing asymmetry (sawtoothness) and decreasing skewness (peakedness) from 2.6 to 0 Ma at site 677 and site 607. From 2.6 to 1.0 Ma, the same phase couplings that are observed in the insolation record are not observed in the oxygen isotope records. From 1 to 0 Ma, benthic and planktic $\delta^{18}\text{O}$ from ODP site 677 contain the same significant bicoherences as the orbital time series. The observed bicoherences, combined with high linear coherence between orbital forcing and climatic response at orbital frequencies during this time period, indicate that most of the climatic ($\delta^{18}\text{O}$) response to insolation forcing is linear, including the response at 100 kyr. The 100 kyr peak in the $\delta^{18}\text{O}$ spectra shown here is consistent with a linear, resonant response of the climate system to direct eccentricity forcing.

Acknowledgments. The cooperation of Nick Shackleton and Maureen Raymo in providing the isotopic data and the time scales used in this study is greatly appreciated. Andre Berger provided new insolation values and offered valuable suggestions. The careful comments of John Imbrie and Bob Oglesby in reviewing this manuscript were very useful and are appreciated. Alan Mix has provided helpful and thorough comments throughout. Walter Munk, after hearing of this study in its preliminary stages, remarked that a linear, resonant climate response would explain the observations. Steve Elgar's research is supported by the Office of Naval Research (Coastal Sciences and Geology and Geophysics) and the National Science Foundation (Physical Oceanography). This work was supported by National Science Foundation grant OCE-90-12270 (Marine Geology and Geophysics) to Oregon State University.

REFERENCES

- Berger, A., Support for the astronomical theory of climatic change, *Nature*, 268, 44-45, 1977.
- Berger, A., Long-term variations of caloric insolation resulting from the earth's orbital elements, *Quat. Res.*, 9, 139-167, 1978a.
- Berger, A., A simple algorithm to compute long term variations of daily or monthly insolation, *Contrib. 18*, Inst. d' Astron. et de Geophys. G. Lemaitre, Univ. Cath. de Louvain, Louvain-la-Neuve, Belgium, 1978b.
- Berger, A., Long-term variations of daily insolation and Quaternary climatic changes, *J. Atmos. Sci.*, 35, 2362-2367, 1978c.
- Berger, A., The spectral characteristics of pre-Quaternary climatic records, and example of the relationship between the astronomical theory and geosciences, in *Climate and Geosciences*, edited by A. Berger et al., pp. 47-76, Kluwer Academic, Boston, Mass., 1989.
- Berger, A., and M.F. Loutre, New insolation values for the climate of the last 10 million years, *Sci. Rep. 1988/13*, Inst. d'Astron. et de Geophys. G. Lemaitre, Univ. Cath. de Louvain, Louvain-la-Neuve, Belgium, 1988.
- Birchfield, G.E., and R.W. Grumbine, "Slow" physics of large continental ice sheets and underlying bedrock and its relation to the Pleistocene Ice Ages, *J. Geophys. Res.*, 90, 11,294-11,302, 1985.
- Birchfield, G.E., and J. Weertman, A note on the spectral response of a model continental ice sheet, *J. Geophys. Res.*, 83, 4123-4125, 1978.
- Elgar, S., Relationships involving third moments and bispectra of a harmonic process, *IEEE Trans. Acoust. Speech Signal Process.*, 35(12), 1725-1726, 1987.
- Elgar, S., and R.T. Guza, Observations of bispectra of shoaling surface gravity waves, *J. Fluid Mech.*, 161, 425-448, 1985.
- Elgar, S., and R.T. Guza, Statistics of bicoherence, *IEEE Trans. Acoust. Speech Signal Process.*, 36(10), 1667-1668, 1988.
- Elgar, S., and G. Sebert, Statistics of bicoherence and biphasic, *J. Geophys. Res.*, 94, 10,993-10,998, 1989.
- Hasselmann, K., Stochastic climate models, Part 1: Theory, *Tellus*, 28, 473-485, 1976.
- Hasselmann, K., W. Munk, and G. MacDonald, Bispectra of ocean waves, in *Time Series Analysis*, edited by M. Rosenblatt, pp. 125-139, John Wiley, New York, 1963.
- Haubrich, R., Earth noises, 5 to 500 millicycles per second, 1, *J. Geophys. Res.*, 70, 1415-1427, 1965.
- Hays, J.D., J. Imbrie, and N.J. Shackleton, Variations in the earth's orbit: pacemaker of the Ice Ages, *Science*, 194, 1121-1132, 1976.
- Imbrie, J., and J.Z. Imbrie, Modeling the climatic response to orbital variations, *Science*, 207, 943-953, 1980.
- Imbrie, J., J.D. Hays, D.G. Martinson, A. McIntyre, A.C. Mix, J.J. Morley, N.G. Pisias, W.L. Prell, and N. Shackleton, The orbital theory of Pleistocene climate: Support from a revised chronology of the marine $\delta^{18}\text{O}$ record, in *Milankovitch and Climate*, edited by A. Berger et al., pp. 269-305, D. Riedel, Norwell, Mass., 1984.
- Imbrie, J., A. McIntyre, and A. Mix, Oceanic response to orbital forcing in the late Quaternary: observational and experimental strategies, in *Climate and Geosciences*, edited by A. Berger et al., pp. 121-163, Kluwer Academic, Boston, Mass., 1989.
- Kim, Y.C., and E.J. Powers, Digital bispectral analysis and its applications to nonlinear wave interactions, *IEEE Trans. Plasma Sci.*, PS-7(2), 120-131, 1979.
- Kim Y.C., J.M. Beall, and E.J. Powers, Bispectrum and nonlinear wave coupling, *Phys. Fluids*, 23(2), 258-263, 1980.
- Le Treut, H., and M. Ghil, Orbital forcing, climatic interactions, and glaciation cycles, *J. Geophys. Res.*, 88, 5167-5190, 1983.
- Maasch, K.A., and B. Saltzman, A low-order dynamical model of global climatic variability over the full Pleistocene, *J. Geophys. Res.*, 95, 1955-1963, 1990.
- Masuda, A., and Y-Y Kuo, A note on the imaginary part of bispectra, *Deep Sea Res.*, 28A(3), 213-222, 1981.
- Matteucci, G., Orbital forcing in a stochastic resonance model of the Late Pleistocene climatic variations, *Clim. Dyn.*, 3, 179-190, 1989.
- Nikias, C.L., and M.R. Raghuveer, Bispectrum estimation: A digital signal processing framework, *Proc. IEEE*, 75, 869-891, 1987.
- Oerlemans, J., Glacial cycles and ice sheet modelling, *Clim. Change*, 4, 353-374, 1982.
- Peltier, R., Dynamics of the ice age earth, *Adv. Geophys.*, 24, 1-146, 1982.
- Pisias, N.G., and T.C. Moore, Jr., The evolution of Pleistocene climate: a time series approach, *Earth Planet. Sci. Lett.*, 52, 450-458, 1981.
- Pisias, N.G., A.C. Mix, and R. Zahn, Nonlinear response in the global climate system: evidence from benthic oxygen isotopic record in core RC13-110, *Paleoceanography*, 5(2), 147-160, 1990.
- Pollard, D., A coupled climate-ice sheet model applied to the Quaternary ice ages, *J. Geophys. Res.*, 88, 7705-7718, 1983.
- Raymo, M.E., W.F. Ruddiman, J. Backman, B.M. Clement, and D.G. Martinson, Late Pliocene variation in Northern Hemisphere ice sheets and North Atlantic Deep Water circulation, *Paleoceanography*, 4(4), 413-446, 1989.
- Ruddiman, W.F., and M.E. Raymo, Northern Hemisphere climate regimes during the past 3 Ma: possible tectonic connections, *Philos. Trans. R. Soc. London, Ser. B*, B318, 411-430, 1988.
- Ruddiman, W.F., M.E. Raymo, D.G. Martinson, B.M. Clement, and J. Backman, Pleistocene evolution: Northern Hemisphere ice sheets and North Atlantic Ocean, *Paleoceanography* 4(4), 353-412, 1989.
- Saltzman, B., Paleoclimatic modeling, in *Paleoclimatic Analysis and Modeling*, edited by A.D. Hecht, pp. 341-396, John Wiley, New York, 1985.
- Saltzman, B., and K.A. Maasch, Carbon cycle instability as a cause of the late Pleistocene Ice Age oscillations: Modeling the asymmetric response, *Global Biogeochem. Cycles*, 2(2), 177-185, 1988.

- Saltzman, B., and A. Sutera, A model of the internal feedback system involved in late Quaternary climatic variations, *J. Atmos. Sci.*, 41(5), 736-745, 1984.
- Saltzman, B., A.R. Hansen, and K.A. Maasch, The late Quaternary glaciations as the response of a three-component feedback system to earth-orbital forcing, *J. Atmos. Sci.*, 41(23), 3380-3389, 1984.
- Shackleton, N.J., and M.A. Hall, Stable isotope history of the Pleistocene at ODP Site 677, edited by K. Becker, et al., *Proc. Ocean Drill. Program Sci. Results*, 111, 295-316, 1989.
- Shackleton, N.J., A. Berger, and W.R. Peltier, An alternative astronomical calibration of the Lower Pleistocene timescale based on ODP Site 677, *Trans. R. Soc. Edinburgh Earth Sci.*, 81(4), 251-261, 1990.
- Sneider, R.K., The origin of the 100,000 year cycle in a simple ice age model, *J. Geophys. Res.*, 90, 5661-5664, 1985.
- Wigley, T.M.L., Spectral analysis and the astronomical theory of climatic change, *Nature*, 264, 629-631, 1976.
-
- S. Elgar, Department of Electrical Engineering and Computer Science, Washington State University, Pullman WA, 99164-2752
- T. Hagelberg and N. Pisias, College of Oceanography, Oregon State University, Ocean Administration Building 104, Corvallis, OR 97331-5503.
- (Received April 24, 1991;
revised August 29, 1991;
accepted August 30, 1991.)